

A Comparison of Damage Detection Methods Applied to Civil Engineering Structures

Szymon Gres¹(✉), Palle Andersen², Rasmus Johan Johansen³,
Martin Dalgaard Ulriksen³, and Lars Damkilde⁴

¹ Department of Structural Engineering, Aalborg University,
Universal Foundation A/S, Aalborg, Denmark
sg@civil.aau.dk

² Structural Vibration Solutions, Aalborg, Denmark

³ Department of Structural and Offshore Engineering,
Aalborg University, Esbjerg, Denmark

⁴ Department of Structural Engineering, Aalborg University, Aalborg, Denmark

Abstract. Facilitating detection of early-stage damage is crucial for in-time repairs and cost-optimized maintenance plans of civil engineering structures. Preferably, the damage detection is performed by use of output vibration data, hereby avoiding modal identification of the structure. Most of the work within the vibration-based damage detection research field assumes that the unmeasured excitation signal is time-invariant with a constant covariance, which is hardly achieved in practice. In this paper, we present a comparison of a new Mahalanobis distance-based damage detection method with the well-known subspace-based damage detection algorithm robust to changes in the excitation covariance. Both methods are implemented in the modal analysis and structural health monitoring software ARTeMIS, in which the joint features of the methods are concluded in a control chart in an attempt to enhance the damage detection resolution. The performances of the methods and their fusion are evaluated in the context of ambient vibration signals obtained from, respectively, numerical simulations on a simple chain-like system and a full-scale experimental example, namely, the Dogna Bridge. The results reveal that the performances of the two damage detection methods are quite similar, hereby evidencing the justification of the new Mahalanobis distance-based approach as it is less computational complex. The control chart presents a comprehensive overview of the progressively damaged structure.

Keywords: Structural health monitoring · Ambient excitation · Damage detection · Control chart-based algorithm fusion

1 Introduction

In the field of damage diagnosis, the vibration-based methods have proven effective in detection of structural deterioration solely based on the operational data from the structure [1]. The practical aspect of using only the output measurements cause several difficulties due to the variations in the ambient excitation, which can be due to variability in environmental conditions, for example, wind, temperature and precipitation,

and operational conditions [2]. This issue is addressed in several detection techniques available in the literature [2–7] and used for the condition-based maintenance and the early damage detection in practice [5]. A general review of different damage detection strategies is presented in [8, 9].

The concept of vibration-based damage detection relates to identification of the damage-induced deviations in the damage-sensitive features of the collected output data. The deviations are defined by a relative comparison of the reference and operational states of the system. The commonly used features for the detection are the modal parameters (natural frequencies, mode shapes and damping ratios) identified from the data. However, some research questions the use of the modal parameters, arguing that the modal data itself is not sensitive enough to detect the local faults [9], especially when in practice the structure is excited by low-frequency inputs. One workaround for the system identification when estimating the features is to use the statistical properties of the data. The statistical methods use the probability distributions of the deviations, which differ between the damaged and the undamaged states, hence indicating faults in the system.

The focus of this work is twofold. One is to present a simple statistical approach for the damage detection based on the Mahalanobis distance featured with the Hankel matrices. The distance metric is calculated on the output vibration data processed in the framework similar to subspace-based methods [12], hereby providing an approach that is robust to changes in the excitation covariance. As such, damage is detected as deviations of the distance from the reference test state. The deviations are compared with the χ^2 -test build on the residual from the subspace-based methods [13]. The second objective is to present a complete, practical overview of the damage indicators combined from both methods in the Hotelling control chart [18].

The performance of both methods is tested on numerical simulations and data from a full-scale bridge. The numerical, academic example is a coupled spring-mass system, excited by white noise of random variance. The full-scale case is the Dogna Bridge, Italy. The bridge is artificially progressively damaged and excited by the wind.

The structure of the paper is as follows. The basic principles of the robust subspace-based damage detection method and the methodology based on the Mahalanobis distance calculated on the Hankel matrices are presented in Sect. 2. The two test examples are described in Sect. 3. Both the comparison and joint performance of the methods on the numerical and full scale detection cases are presented in Sect. 4. The results are concluded in Sect. 5.

2 Methodology

In this section we recall the basic principles of the subspace-based damage detection [7] and present the algorithm for the Mahalanobis distance-based damage detection. Both methods are data-driven.

2.1 Subspace-Based Damage Detection

The damage detection consists of monitoring the deviations of the current system from its reference state, characterized by some nominal property repeatable for every

healthy conditions. The deviations are defined by a residual that, theoretically, differs between the healthy and the damaged states [13]. Consider the discrete state space model

$$\begin{aligned} \mathbf{x}_{k+1} &= \mathbf{F}\mathbf{x}_k + \mathbf{v}_k \\ \mathbf{y}_k &= \mathbf{H}\mathbf{x}_k + \mathbf{w}_k \end{aligned} \tag{1}$$

with the state transition matrix $\mathbf{F} \in R^{n \times n}$, the observation matrix $\mathbf{H} \in R^{r \times n}$, the states $\mathbf{x}_k \in R^n$ and the outputs $\mathbf{y}_k \in R^r$, where r is the number of sensors and n denotes the order of the system [6]. The unmeasured white noise input \mathbf{v}_k drives the dynamics of the system and \mathbf{w}_k is the measurement noise. Any perturbation in the structural properties of the system, manifested in the stiffness or mass, leads to deviations in the state matrices and are subsequently reflected in \mathbf{y}_k . As a consequence, damage changes the eigenstructure of the state space model. Hence, the damage-sensitive system property relates to \mathbf{F} .

Let $\Sigma_s = E(\mathbf{x}_{k+1}\mathbf{x}_{k+1}^T)$ be the state covariance matrix and $\mathbf{G} = E(\mathbf{x}_{k+1}\mathbf{y}_k^T) = \mathbf{F}\Sigma_s\mathbf{H}^T$ the cross-covariance between the states and the outputs [6]. The output covariance yields $\Lambda_i = E(\mathbf{y}_{k+i}\mathbf{y}_k^T) = \mathbf{H}\mathbf{F}^{i-1}\mathbf{G}$ and can be structured in the block-Hankel matrix

$$\mathbf{H}_{p+1,q} = \begin{bmatrix} \Lambda_1 & \Lambda_2 & \dots & \Lambda_q \\ \Lambda_2 & \Lambda_3 & \dots & \Lambda_{q+1} \\ \vdots & \vdots & \ddots & \vdots \\ \Lambda_{p+1} & \Lambda_{p+2} & \dots & \Lambda_{p+q} \end{bmatrix} = \text{Hank}(\Lambda_i). \tag{2}$$

$\mathbf{H}_{p+1,q} \in R^{(p+1)r \times qr}$ where p and q are parameters such $q = p + 1$. The $\mathbf{H}_{p+1,q}$ can be factorized into the observability and controllability matrices such

$$\mathbf{H}_{p+1,q} = \mathbf{O}_{p+1,q}\mathbf{C}_q \tag{3}$$

where the observability matrix, $\mathbf{O}_{p+1,q} \in R^{(p+1)r \times n}$, and controllability matrix, $\mathbf{C}_q \in R^{n \times qr}$, are given by

$$\mathbf{O}_{p+1,q} = \begin{bmatrix} \mathbf{H} \\ \mathbf{HF} \\ \vdots \\ \mathbf{HF}^p \end{bmatrix}, \mathbf{C}_q = [\mathbf{G} \quad \mathbf{FG} \quad \dots \quad \mathbf{F}^{q-1}\mathbf{G}]. \tag{4}$$

The subspace-based damage detection test detects if the residual of the characteristic property of the reference (healthy) state of the system based on $\mathbf{O}_{p+1,q}$, or subsequently $\mathbf{H}_{p+1,q}$ (Eq. 5), is significantly different from zero. Consider the space, or a property of the reference state, where

$$\mathbf{S}^T \hat{\mathbf{H}}_{p+1,q} \approx 0. \tag{5}$$

$\hat{\mathbf{H}}_{p+1,q}$ is the empirical output block-Hankel matrix and \mathbf{S} is the left kernel \mathbf{U}_0 of the reference state $\hat{\mathbf{H}}_{p+1,q}$, hence

$$\hat{\mathbf{H}}_{p+1,q}^{ref} = [\mathbf{U}_1 \quad \mathbf{U}_0] \begin{bmatrix} \Delta_1 & 0 \\ 0 & \Delta_0 \end{bmatrix} \begin{bmatrix} \mathbf{V}_1^T \\ \mathbf{V}_0^T \end{bmatrix}, \quad (6)$$

where Δ_1 contains non-zero singular values. The reference and the subsequently tested states share the same left null space only when no damage occurs. Bearing that in mind, the residual vector is defined as

$$\xi = \sqrt{N} \text{vec}(\mathbf{S}^T \hat{\mathbf{H}}_{p+1,q}). \quad (7)$$

Note that the excitation of the system is ambient, which leads to changes in the cross-covariance matrix, \mathbf{G} , (recall $\mathbf{G} = \text{E}(\mathbf{x}_{k+1}\mathbf{y}_k^T) = \mathbf{F}\Sigma_s\mathbf{H}^T$), and consequently in the output block Hankel matrix $\hat{\mathbf{H}}_{p+1,q}$. That results in non-zero residuals (Eq. 7) between the healthy states. To avoid that, [13] use the fact that $\hat{\mathbf{H}}_{p+1,q}$ shares the same null space with its principal left singular vectors \mathbf{U}_1 , so for each healthy state it holds that $\mathbf{S}^T\mathbf{U}_1 \approx 0$. Matrix \mathbf{U}_1 contains n independent column vectors that span the column space of $\hat{\mathbf{H}}_{p+1,q}$ and are principal directions of the data, invariant to the change in excitation covariance [19]. The robust residual is defined as

$$\xi = \sqrt{N} \text{vec}(\mathbf{S}^T \mathbf{U}_1), \quad (8)$$

which is tested for being significantly different from zero by use of the χ^2 -test,

$$\chi_{\xi}^2 = \xi^T \Sigma_{\xi}^{-1} \xi, \quad (9)$$

where Σ_{ξ} is the empirical covariance of the residual calculated as in [7].

2.2 Mahalanobis Distance-Based Damage Detection

The Mahalanobis distance, MD, is a metric used in multivariate statistics to calculate the distance between a point and a distribution. The formulation of the metric takes into account the correlations between different data dimensions by the covariance matrix of the data. For the multivariate normally distributed variables, the squared MD follows the χ^2 -distribution [20]. One of its practical uses is detection of outliers [16] and recently detection of structural damages based on the transmissibility functions or AR-coefficients as a feature [14, 15].

The square Mahalanobis metric of the observations in the data vector \mathbf{x}_i , from the reference data vector with the sample mean $\boldsymbol{\mu}$ and the covariance matrix $\boldsymbol{\Sigma}$ is defined as

$$MD_i = (\mathbf{x}_i - \boldsymbol{\mu})^T \boldsymbol{\Sigma}^{-1} (\mathbf{x}_i - \boldsymbol{\mu}). \quad (10)$$

In this paper the Mahalanobis distance is calculated on the empirical block-Hankel matrices with the output correlations between a reference and damaged states and used

directly as a damage indicator. The proposed metric is robust towards the variations of the excitation covariance and can therefore be used with the operational measurements. Consider m reference data sets and i tested states, so that

$$\begin{aligned} MD_i \leq T_m &\rightarrow \text{healthy} \\ MD_i > T_m &\rightarrow \text{damaged} \end{aligned}$$

where T_m is a threshold calculated for the reference state. The MD increases as the system is subjected to any change that affects its vibration characteristics. The modified version of the squared MD featured with the Hankel matrices is defined as

$$MD_i = \text{vec}(\hat{\mathbf{H}}_{p+1,q}^{corr})^T \left(\Sigma_{\hat{\mathbf{H}}_{p+1,q}^{corr.ref}} \right)^{-1} \text{vec}(\hat{\mathbf{H}}_{p+1,q}^{corr}). \tag{11}$$

Let $Y \in R^{r \times mN}$ where Y is the output response, m is the number of the reference sets and N is the length of one data set. The formulation of the empirical block-Hankel matrix yields

$$\hat{\mathbf{C}}_i = \frac{1}{mN} \sum_{k=1}^{mN} \frac{\mathbf{Y}_k \mathbf{Y}_{k-i}^T}{\sigma_k \sigma_{k-i}}; \hat{\mathbf{H}}_{p+1,q}^{corr.ref} = \text{Hank}(\hat{\mathbf{C}}_i). \tag{12}$$

Consequently, $\hat{\mathbf{H}}_{p+1,q}^{corr}$ is determined using Eq. 12 for each tested data set with $m = 1$. The covariance of the empirical, vectorized Hankel matrix is estimated from the covariance of the sample mean with the methodology recalled from [7]. The threshold above which the data set is considered damaged is defined as one standard deviation above the mean value of the reference state, which theoretically should approach zero.

2.3 Simple System Simulation

For the numerical test, we considered a coupled spring-mass system with 15 DOF, Fig. 1. Output accelerations are simulated using white noise input of variance taken randomly from the normally distributed vector in between [1 50], acting on the last DOF. The acceleration data is recorded in all DOF along the system. To challenge the robustness of the damage detection methods, different amounts of white noise, namely, 3%, 10% and 30%, are added to the response signals.

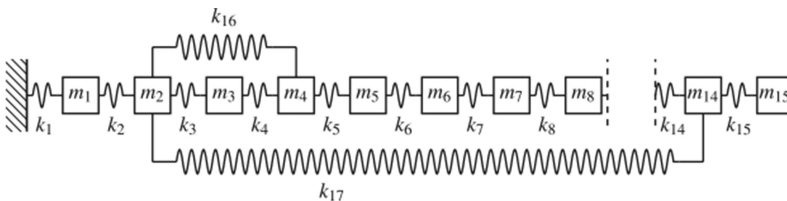


Fig. 1. Simple system scheme.

The damage is simulated as a progressive reduction in the stiffness of the 8th spring by 2%, 5%, 10% and 30%. The sampling frequency is 50 Hz. The system is excited for 1000 s in blocks of 50 data sets for each simulated case. That results in 250 data records per sensor per noise level with a random variance in between each set.

3 Results

The damage is detected for the three noise levels present in the response of the simple system. 30 out of 50 healthy data sets are used to establish the reference state. The thresholds for both of the methods are defined as a number of standard deviations above the mean metric of the reference state. One standard deviation for the unsafe zone, and two standard deviations for the damaged zone.

The comparison of the damage indicators for the case of 3% and 30% of white noise added to the response data is illustrated in Figs. 2 and 3. The percentage of the detected damage sets with respect to the simulation case and degree of the damage is summarized in the Table 1.

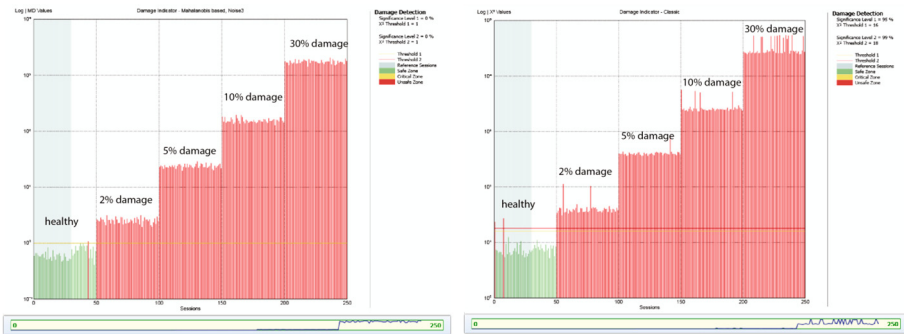


Fig. 2. Damage detection in simple system. Case-3% of noise in the response. Damage indicators for the Mahalanobis-based (left) and robust subspace-based (right).

Both methods are robust towards the change in variance of the excitation and detect each degree of the damage present in the response data containing 3% of white noise, Fig. 2. While increasing the noise level to 30%, the Mahalanobis-based approach performs more accurate in detecting the smaller deviations, see Fig. 3 and Table 1. The fusion of the methods in a control chart, created for the 30% noise case, results in detection of all the 5% damage sets and half of the 2% damaged sets; what was not possible with a single method, see Fig. 4.

4 Dogna Bridge

The Dogna bridge, Fig. 5, crosses the River Fella and connects the villages of Crivera and Valdogna (Dogna) in Friuli Venezia Giulia, a region located in the North East of Italy.

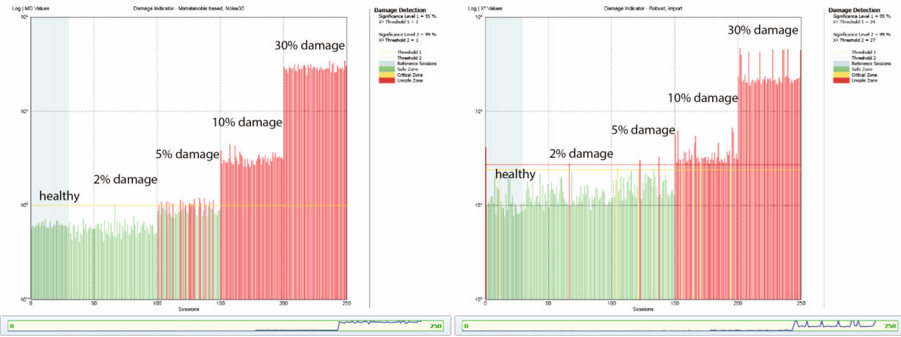


Fig. 3. Damage detection in simple system. Case-30% of noise in the response. Damage indicators for the Mahalanobis-based (left) and robust subspace-based (right).

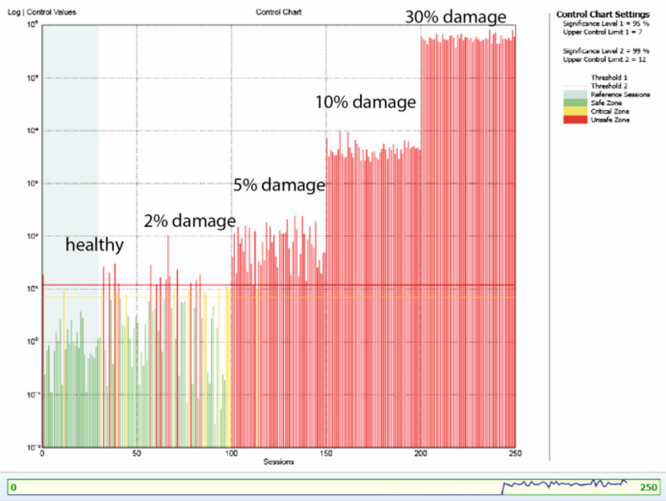


Fig. 4. Hotelling T^2 control chart for simple system. Robust subspace and Mahalanobis-based detection. Case: noise 30%.

Table 1. Comparison of the detection methods. Ability to detect damage in the simple system for different noise levels.

Case	Method	Damaged sets detected			
		2% damage	5% damage	10% damage	30% damage
Noise 3%	Subspace-based	100%	100%	100%	100%
	Mahalanobis-based	100%	100%	100%	100%
Noise 10%	Subspace-based	10%	26%	100%	100%
	Mahalanobis-based	40%	100%	100%	100%
Noise 30%	Subspace-based	2%	8%	100%	100%
	Mahalanobis-based	0%	40%	100%	100%

The bridge is a four-span, single-lane concrete bridge. The span is 16 m, with a 4 m lane. The deck is made of a 0.18 m reinforced concrete (RC) slab, supported by three longitudinal simply supported RC beams with a rectangular cross-section of 0.35×1.20 m. The beams are connected to the supports with the rectangular RC



Fig. 5. Dogna bridge, Italy.

diaphragms 0.3×0.7 m. The piers are RC walls 1.5 m thick, 4.5 m deep, and 3.6 m high. The pylons are fixed in a piled foundation that consists of a 1 m thick RC slab supported by a drilled RC piles of 1 m in diameter and 18 m in length.

For traffic safety reasons, the Dogna bridge was demolished on May 2008 and has been replaced by a new bridge built about 200 m downstream. A test campaign was carried out from April 02 to 11 2008 and consisted of a series of tests progressively damaging one of the bridge spans. The tests were carried out under similar environmental conditions so the influence of temperature and humidity on the structure is insignificant. Figure 6 shows the artificially damaged bridge span during the tests.

The bridge was equipped with ten accelerometers mounted on its deck. The samples were taken with the frequency of 400 Hz. The measurement campaign lasted 50 min in total while the reference state was measured for 20 min. The damage was introduced in three blocks: the first cut, the second cut and the third cut with the damaged center span.

5 Results

For the general overview of the measurements, the first six singular values of the cross-spectral densities from the output acceleration data for the reference state are plotted in Fig. 7.

A total number of 22 data sets are analyzed. Each measurement lasts 147.5 s. In the frequency range of 0–40 Hz there are three modes excited at 10.2 Hz, 14.2 Hz and 27.2 Hz, Fig. 7.



Fig. 6. Artificially damaged beams. The cuts introduced progressively during the tests, along with the damage in the centerline of the span.

The reference measurement model for the damage detection is built from 6 out of 8 healthy data records. Data sets between 9 and 14 are the measurements from the damaged state corresponding to the cuts in the beams. Damaged in the centerline was introduced in data sets from 15 to 22. The comparison of the subspace-based and Mahalanobis-based detection methods and the control chart combining the methods is illustrated in Fig. 8.

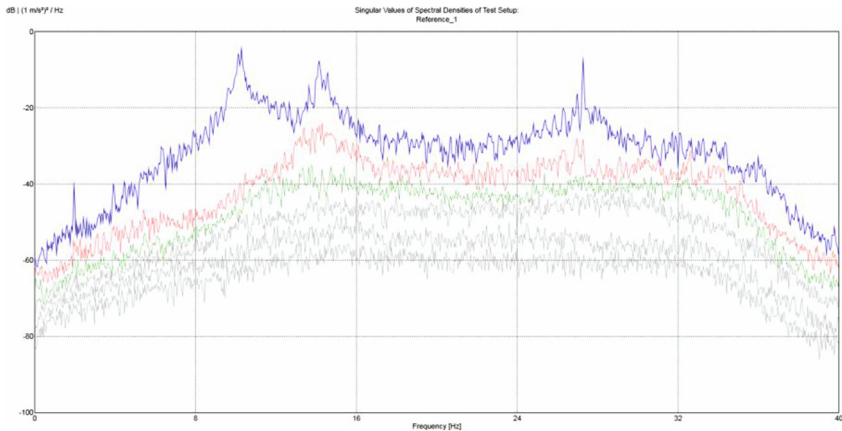


Fig. 7. First six singular values of the cross spectral densities of the output acceleration data for the reference state.

Both the subspace-based and Mahalanobis-based damage indicators do not increase with the number of the cuts in the beams in sets 9–14, see Fig. 8. However, each method clearly distinguishes the healthy data from the damaged and detects the last stage of the damage (the damage of the centerline of the span), see Figs. 6 and 8. In this case, the fusion of the detection methods in the control chart does not enhance the damage detection, however results in similar indicators as obtained from the robust subspace and Mahalanobis distance-based methods.

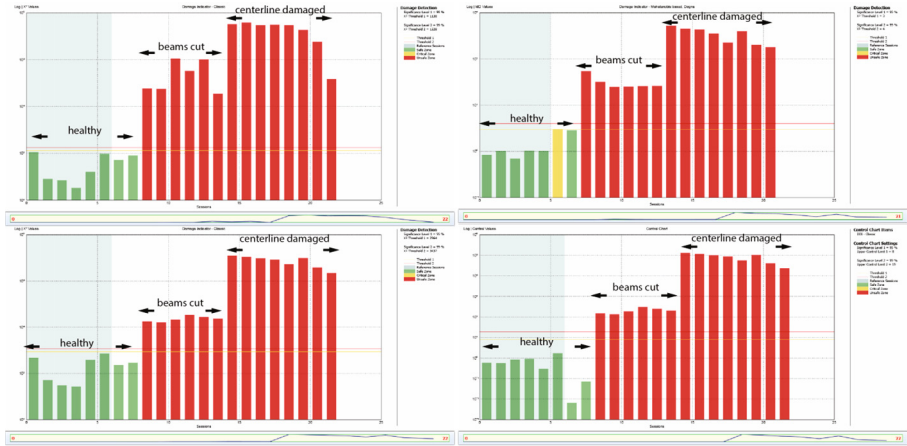


Fig. 8. Damage detection in Dogna bridge. Damage indicators from top: Robust subspace (left). Mahalanobis-based (right). From bottom classical subspace (left), Hotelling control chart (right).

6 Conclusions

In this paper a recently developed Mahalanobis distance-based damage detection method was presented and compared to well-known and proven subspace-based damage detection approaches. The methods were tested on noisy simulation data and a full-scale bridge example. Both test cases were excited by ambient excitation with a changing intensity.

The performance of the new Mahalanobis distance-based detection method appears similar to the subspace-based methods for the low-noise numerical and experimental cases. As well as the subspace-based methods, the proposed algorithm is robust to changes in the excitation covariance. The new method reveals advantage over the subspace-based methods regarding detection of the damages based on the noisy simulations. The combination of the methods in the control chart was successful and resulted in the most effective detection of the damages both for simulations and the full-scale test.

The research regarding the detection methods will continue with focus on testing the algorithms on more extensive full-scale experimental campaigns with different types and extent of damages. The fusion of the methods enhanced the performance of the combined damage indicators, hence research on this subject will proceed. The use of empirical block-Hankel matrices as damage sensitive features will be further examined and compared with different transformation of the output data.

References

1. Farrar, C., Doebling, S., Nix, D.: Vibration-based structural damage identification. *Philos. Trans. R. Soc. A Math. Phys. Eng. Sci.* **359**(1778), 131–149 (2001)
2. Balmès, E., Basseville, M., Mevel, L., Nasser, H.: Handling the temperature effect in vibration-based monitoring of civil structures: a combined sub-space-based and nuisance rejection approach. *Control Eng. Pract.* **17**(1), 80–87 (2009)
3. Bernal, D.: Kalman filter damage detection in the presence of changing process and measurement noise. *Mech. Syst. Signal Process.* **39**(1–2), 361–371 (2013)
4. Döhler, M., Hille, F.: Subspace-based damage detection on steel frame structure under changing excitation. In: *Proceedings of 32nd International Modal Analysis Conference, Orlando* (2014)
5. Döhler, M., Hille, F., Mevel, L., Rücker, W.: Structural health monitoring with statistical methods during progressive damage test of S101 bridge. *Eng. Struct.* **69**, 183–193 (2014)
6. Döhler, M., Mevel, L.: Subspace-based fault detection robust to changes in the noise covariances. *Automatica* **49**(9), 2734–2743 (2013)
7. Döhler, M., Mevel, L., Hille, F.: Subspace-based damage detection under changes in the ambient excitation statistics. *Mech. Syst. Signal Process.* **45**(1), 207–224 (2014)
8. Doebling, S., Farrar, C., Prime, M.: A summary review of vibration-based damage identification methods. *Shock Vib. Dig.* **30**(2), 91–105 (1998)
9. Carden, E., Fanning, P.: Vibration based condition monitoring: a review. *Struct. Health Monit.* **3**(4), 355–377 (2004)
10. Worden, K., Farrar, C., Manson, G., Park, G.: The fundamental axioms of structural health monitoring. *Proc. R. Soc. A Math. Phys. Eng. Sci.* **463**(2082), 1639–1666 (2007)
11. Worden, K., Manson, G., Fieller, N.: Damage detection using outlier analysis. *J. Sound Vib.* **229**(3), 647–667 (2000)
12. Van Overschee, P., De Moor, B.: *Subspace identification for linear systems: theory, implementation, applications.* Kluwer Academic Publisher, Boston (1996)
13. Basseville, M., Abdelghani, M., Benveniste, A.: Subspace-based fault detection algorithms for vibration monitoring. *Automatica* **36**(1), 101–109 (2000)
14. Zhou, Y., Maia, N.M., Wahab, M.A.: Damage detection using transmissibility compressed by principal component analysis enhanced with distance measure. *J. Vib. Control* (2016). doi:[10.1177/1077546316674544](https://doi.org/10.1177/1077546316674544)
15. Cheung, A., Cabrera, C., Sarabandi, P., Nair, K.K., Kiremidjian, A.: The application of statistical pattern recognition methods for damage detection to field data. *Smart Mater. Struct.* **17**, 1–12 (2008)
16. Filzmoser, P.: A multivariate outlier detection method. In: *Proceedings of State University Conference*, 18 (2004)
17. ARTEMIS Pro. 5.1: *Structural Vibration Solutions A/S.* NOVI Science Park, Aalborg (2016)
18. Lowry, C.A., Montgomery, D.C.: A review of multivariate control charts. *IIE Trans.* **27**(6), 800–810 (1995)
19. Yan, A.M., Golinval, J.C.: Null subspace-based damage detection of structures using vibration measurements. *Mech. Syst. Signal Process.* **20**, 611–626 (2006)
20. Hardin, J., Rocke, D.M.: The distribution of robust distances. *J. Comput. Graph. Stat.* **14**(4), 928–946 (2005)